Synthesis and Conformational Studies of a Cyclic Analog of the Proximal Zinc Finger of HIV-1 NCP7 for Antibody Generation

C. Z. Dong, N. Jullian, Y. S. Yang, H. de Rocquigny, M. C. Fournie-Zaluski, and B. P. Roques*

Contribution from the Département de Pharmacochimie Moléculaire et Structurale, INSERM U266, CNRS URA D 1500, UFR des Sciences Pharmaceutiques et Biologiques, Faculté de Pharmacie, 4, avenue de l'Observatoire, 75270 Paris Cedex 06, France

Received June 27, 1994[⊗]

Abstract: The nucleocapsid protein NCp7 of human immunodeficiency virus type 1 (HIV-1) contains two zinc finger domains (CCHC boxes), which have been shown to be very important in the viral replication cycle. However, these domains are not involved directly in either *in vitro* RNA dimerization or $tRNA^{Lys,3}$ annealing. For a more detailed understanding of the role of the zinc fingers in the different functions of NCp7, antibodies directed against these domains would be very useful. For this purpose, a cyclic peptide analog of the proximal zinc finger (13-30)NCp7 has been synthesized in solid phase using a strategy of combined Fmoc and Boc chemistry. On the basis of the 3D structural data of NCp7, the Asn^{17} and Ala^{30} have been changed to Glu^{17} and Lys^{30} and a cyclization carried out between their side chains. The structures of the cyclic and native peptides complexed with Co^{2+} and Zn^{2+} were studied by visible and 2D ^1H NMR spectroscopy, respectively. The nuclear Overhauser effects obtained were applied as constraints to determine the solution structures using DIANA software followed by AMBER energy refinement. The results show that the cyclic peptide retains the highly folded structure of the native peptide and exhibits an enhanced affinity for metallic ions. These are favorable parameters for the generation of antibodies against the zinc fingers in NCp7.

Introduction

The nucleocapsid protein NCp15, a maturation product of the gag precursor of the human immunodeficiency virus type 1 (HIV-1), is a major core structural protein of the virion.[1,2] The processing of NCp15 gives rise to two peptide fragments p6 and NCp7,[3] a 72 amino acid protein which retains all the *in vitro* biological activities of the entire protein.[4,5] NCp7 has been shown to induce *in vitro* RNA dimerization and annealing of the primer $tRNA^{Lys,3}$ to the RNA initiation site of the reverse transcription.[4-7] NCp7 contains two zinc fingers of the type $CX_2CX_4HX_4C$[8] linked together by a short sequence RAPRKKG. These finger domains bind zinc with a high affinity ($k_{app} \sim 10^{13}$ M^{-1})[9,10] and seem to play a crucial role in the virus life cycle, since point mutations of the zinc chelating amino acids[11,12] or deletion of the entire fingers led to a noninfectious virus.[13,14] However, *in vitro* experiments have shown that these fingers are not directly involved in either RNA dimerization or $tRNA^{Lys,3}$ annealing.[7]

To clarify the functions of the finger domains, a structural analysis of NCp7 has been performed by ^1H NMR spectroscopy.[15-17] It has been shown that the sequences 15-28 and 36-49, corresponding to the proximal and distal fingers, respectively, are highly folded around the zinc ion.[18,19] Furthermore, a spatial proximity between these two domains has been evidenced by a set of NOEs between the two fingers and between the fingers and the linker region.[16,20] This temperature-dependent[16] conformation of NCp7 was not observed in other studies.[15,17] This could be due to differences in the conditions of NMR studies (concentration of NCp7, pH, temperature, etc.) as recently discussed in detail.[12,20] However, the biological significance of this internally folded conformation of NCp7 has

* To whom correspondence should be addressed.

⊗ Abstract published in *Advance ACS Abstracts*, February 15, 1995.

(1) Barré-Sinoussi, F.; Chermann, J. C.; Rey, F.; Nugeyre, M. T.; Chamaret, S.; Gruest, J.; Dauguet, C.; Axler-Blin, C.; Vézinet-Brun, F.; Rouzioux, C.; Rozenbaum, W.; Montagnier, L. *Science* **1983**, *220*, 868-870.

(2) Ratner, L.; Haseltine, W.; Patorca, R.; Livak, K. J.; Starcich, B.; Josephs, S. F.; Doran, E. R.; Rafalski, J. A.; Whitehorn, E. A.; Baumeister, K.; Ivanoff, L.; Petteway, S. R., Jr.; Pearson, M. L.; Lautenberger, J. A.; Papas, T. S.; Ghrayeb, J.; Chang, N. T.; Gallo, R. C.; Wong-Staal, F. *Nature* **1985**, *313*, 277-284.

(3) DiMarzo Véronese, F.; Rhaman, R.; Copeland, T. D.; Oroszland, S.; Gallo, R. C.; Sarnjadharm, M. G. *AIDS Res. Hum. Retroviruses* **1987**, *3*, 253-264.

(4) Darlix, J. L.; Gabus, C.; Nugeyre, M. T.; Clavel, F.; Barré-Sinoussi, F. *J. Mol. Biol.* **1990**, *216*, 689-699.

(5) de Rocquigny, H.; Ficheux, D.; Gabus, C.; Fournié-Zaluski, M. C.; Darlix, J. L.; Roques, B. P. *Biochem. Biophys. Res. Commun.* **1991**, *180*, 1010-1018.

(6) Prats, A. C.; Sarih, L.; Gabus, C.; Listvak, S.; Keith, G.; Darlix, J. L. *EMBO J.* **1988**, *7* (6), 1777-1783.

(7) de Rocquigny, H.; Gabus, C.; Vincent, A.; Fournié-Zaluski, M. C.; Roques, B. P.; Darlix, J. L. *Proc. Natl. Acad. Sci.* **1992**, *89*, 6472-6476.

(8) Berg, J. M. *Science* **1986**, *232*, 485-487.

(9) Green, L. M.; Berg, J. M. *Proc. Natl. Acad. Sci.* **1990**, *87*, 6403-6407.

(10) Mély, Y.; Cornille, F.; Fournié-Zaluski, M. C.; Darlix, J. L.; Roques, B. P.; Gérard, D. *Biopolymers* **1991**, *31*, 899-906.

(11) Aldovini, A.; Young, R. A. *J. Virol.* **1990**, *64*, 1920-1926.

(12) Déméné, H.; Dong, C. Z.; Rouyez, M. C.; Ruffault, A.; Jullian, N.; Morellet, N.; Mély, Y.; Ottmann, M.; Darlix, J. L.; Fournié-Zaluski, M. C.; Saragosti, S.; Roques, B. P. *Biochemistry* **1994**, *33*, 11707-11716.

(13) Gorelick, R. J.; Nigida, S. M., Jr.; Bess, J. W., Jr.; Arthur, L. O.; Henderson, L. E.; Rein, A. *J. Virol.* **1990**, *64*, 3207-3211.

(14) Gorelick, R. J.; Chabot, D. J.; Rein, A.; Henderson, L. E.; Arthur, L. O. *J. Virol.* **1993**, *67*, 4027-4036.

(15) Omichinski, J. G.; Clore, G. M.; Sakaguchi, K.; Appella, E.; Gronenborn, A. M. *FEBS Lett.* **1991**, *292*, 25-30.

(16) Morellet, N.; Jullian, N.; de Rocquigny, H.; Maigret, B.; Darlix, J. L.; Roques, B. P. *EMBO J.* **1992**, *11*, 3059-3065.

(17) Summers, M. F.; Henderson, L. E.; Chance, M. R.; Gess, J. W., Jr.; South, T. L.; Blake, P. R.; Sagi, I.; Perez-Alvardo, G.; Sowder, R. C., III; Hare, D. R.; Arthur, L. O. *Protein Sci.* **1992**, *1*, 563-574.

(18) Summers, M. F.; South, T. L.; Kim, B.; Hare, D. R. *Biochemistry* **1990**, *29*, 329-340.

(19) South, T. L.; Blake, P. R.; Hare, D. R.; Summers, M. F. *Biochemistry* **1991**, *30*, 6342-6349.

(20) Morellet, N.; de Rocquigny, H.; Mély, Y.; Jullian, N.; Déméné, H.; Ottmann, M.; Gérard, D.; Darlix, J.-L.; Fournié-Zaluski, M. C.; Roques, B. P. *J. Mol. Biol.* **1994**, *235*, 287-301.

0002-7863/95/1517-2726$09.00/0

been established *ex vivo* and *in vivo* by point mutations which modified the relative orientations of the finger domains or the 3D structure of the proximal finger.[12,20] Thus, the replacement of Pro^{31}, which is responsible for the close proximity of the fingers, by a leucine residue led to an immature virion which does not contain reverse transcriptase.[12] Likewise, the replacement of the zinc chelating His^{23} residue by a cysteine led to a finger domain which was still able to complex zinc, but the mutation induced a conformational change of the protein and a reduction in affinity for RNA.[12] In the virus genome this mutation produced a loss of infectivity, probably due to encapsidation of degraded RNA.[12]

All these data reflect the importance of the finger domains of NCp7 in various steps of the virus life cycle. To elucidate more effectively the different functions of NCp7 *in vivo* and the role of the finger domains, antibodies directed against NCp7 have been generated in mice or rats. By this strategy, 18 monoclonal antibodies were isolated and tested for their epitopic specificity by classical Elisa tests.[21] Three families of antibodies recognized continuous epitopes in the N- and C-terminal parts of the proteins and the two others noncontinuous epitopes. However, none of these antibodies was directed against the zinc fingers.

In order to overcome this problem, a cyclic analog of the proximal zinc finger (13−30)NCp7 has been synthesized, based on the 3D structure of this domain in NCp7 and studied using ^1H NMR spectroscopy and molecular modeling.[16] We report in this paper the synthesis of this cyclic peptide, the comparison of its tridimensional structure with that of the native finger, and its improved affinity for metal ions.

Materials and Methods

Peptide Synthesis. Piperidine, *N*-methylpyrrolidone (NMP), dichloromethane (DCM), dicyclohexylcarbodiimide (DCC), 1-hydroxybenzotriazole (HOBt), and some Fmoc-protected amino acids [Ala, Gly, Phe, Pro, Val, Asn(trt), His(trt), Glu(*t*Bu), Lys(Boc)] were purchased from Applied Biosystems. The other Fmoc-protected amino acids [Arg(tos), Cys(4MeBzl), Glu(OcHex), Lys(2ClZ), Thr(Bzl)] and trifluoroacetic acid (TFA) were purchased from Neosystem Laboratory (Strasbourg, France). 1,2-Ethanedithiol (EDT) and *m*-cresol were obtained from Aldrich Chimie (Paris, France), 4-((2′,4′-dimethoxyphenyl)(fmoc)-aminomethyl)phenoxy resin was obtained from Novabiochem (France), and HF was obtained from Satic (France).

Assembly of the protected peptide was carried out according to the stepwise solid phase method of Merrifield[22] on an Applied Biosystems 431A peptide synthesizer, using a longer coupling time (45 min) and DCC/HOBt as coupling reagents. The amino acids were side-chain-protected as indicated above (Figure 2). At the end of the synthesis, the peptidyl resin was treated for 1 h with 80 mL of TFA in the presence of EDT (2.0 mL) and water (2.0 mL) to remove the resin and deprotect the side chains of Glu^{17} and Lys^{30}. After evaporation of TFA, the peptide was precipitated by cold ether and collected by centrifugation (4000 rpm × 10 min). The pellet was dissolved in TFA (6 mL), and the precipitation by ether and the centrifugation were repeated once more. The peptide was then solubilized in a mixture of CH_3CN and water. After evaporation of CH_3CN, the peptide was lyophilized and used directly without further purification. Cyclization was performed in DMF (~2 mM) with BOP/HOBt (3 equiv each) as coupling reagents in the presence of diisopropylethylamine (DIEA, 4 equiv) overnight.[23] After a volume reduction, the protected cyclic peptide was precipitated with a solution of $NaHCO_3$ (saturated) and washed 3 times with water.

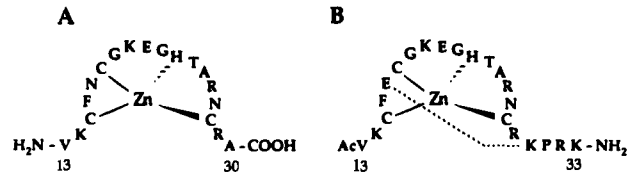

Figure 1. Primary structures of the proximal zinc finger of HIV-1 NCp7 [(13−30)NCp7] (A) and its cyclic analog [c[Glu^{17}, Lys^{30}(13−33)NCp7]] (B). The cyclization bond is indicated with a dashed line.

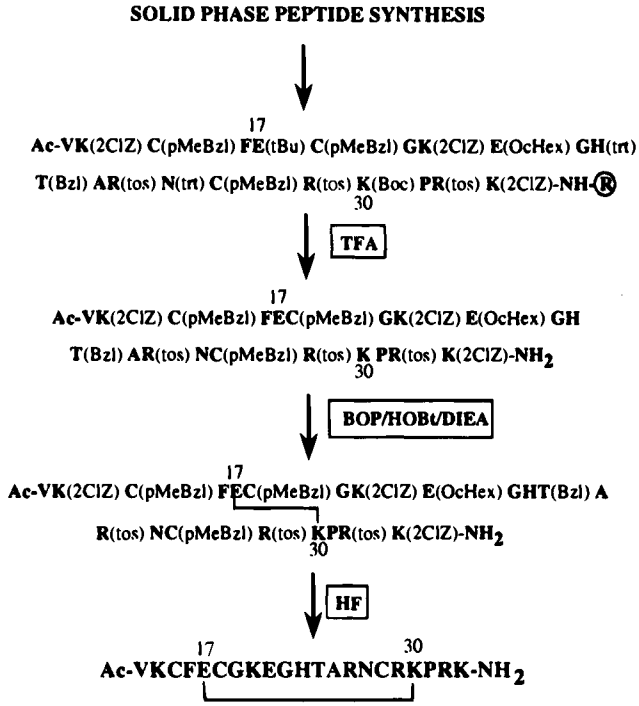

Figure 2. Scheme for the synthesis of the cyclic peptide c[Glu^{17}, Lys^{30}-(13−33)NCp7].

Finally, the peptide was dissolved in a mixture of CH_3CN and water. After evaporation of CH_3CN and lyophilization, the protecting groups of the cyclic peptide were cleaved by HF (10 mL) for 1 h at 0 °C in the presence of *m*-cresol (1.0 mL). HF then was evaporated and the final product was precipitated with cold ether. The crude peptide was dissolved in water, lyophilized, and purified by HPLC with a C18 Vydac column (5 μm, 220 × 10 mm), using a linear gradient of 0−30% B in 90 min (where A, 0.1% TFA/H_2O; B, 70% CH_3CN/30% H_2O/0.09% TFA) at a flow rate of 1.5 mL min^{-1} with detection at 214 nm. The purity of the final product was checked under isocratic conditions on analytical HPLC, using a Vydac C4 column and 10% CH_3CN/90% NH_4Ac, 50 mM as eluant. Its identify has been confirmed by electrospray mass spectroscopy and amino acid analysis. Moreover, only the peaks corresponding to the cyclic peptide could be detected in the 600 MHz ^1H NMR spectrum.

UV Measurements. (13−30)NCp7 and its cyclic analog c[Glu^{17},-Lys^{30}(13−33)NCp7] were dissolved in 50 mM HEPES, 0.1 M KCl buffer (pH 7.5) in the presence of 1.0 equiv of cobalt chloride. Visible absorption spectra were obtained with a Perkin-Elmer spectrometer (Lambda 3B). In competition experiments, a solution of EGTA (10 equiv) was rapidly added to the Co^{2+}−peptide (1:1) solution. The dissociation curves were recorded directly with an associated computer. To evaluate the affinity of the peptide for cobalt by this method, a titration experiment with increasing quantities of EGTA to the Co^{2+}−peptide complex (1:1) was performed. Each point was determined when the reaction had reached equilibrium.

NMR Experiments. The cyclic zinc finer, c[Glu^{17},Lys^{30}(13−33)-NCp7], was dissolved at a concentration of 2.0 mM, in 90% H_2O, 10% D_2O in the presence of 1.5 equiv of zinc chloride. The pH was adjusted to 5.6 ± 0.1 with small aliquots of 1M NaOD or 1M DCl.

All the NMR spectra were recorded on a Bruker AMX 600 spectrometer at 293 K, with 512 × 2048 data points. The TOCSY

(21) Tanchou, V.; Delauney, T.; de Rocquigny, H.; Darlix, J. L.; Bodeus, M.; Roques, B. P.; Benarous, R. *AIDS Res. Hum. Retroviruses* **1994**, *10*, 983−993.

(22) Barany, G.; Merrifield, R. B. *Peptides*; Gross, E., Ed.; J. Heirnhsfer: New York, 1979; pp 1−224.

(23) McMurray, J. S.; Budde, R. J. A.; Dyckes, D. F. *Int. J. Pept. Protein Res.* **1993**, *42*, 209−215.

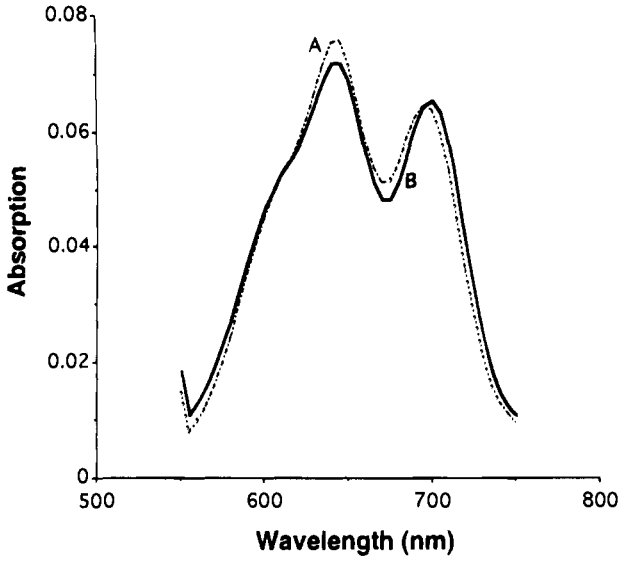

Figure 3. Visible absorption spectra of $Co^{2+}-(13-30)$NCp7 (A) and $Co^{2+}-c[Glu^{17}, Lys^{30}(13-33)NCp7]$ (B) in 50 mM Hepes, 0.1 M KCl at pH 7.5 and 293 K.

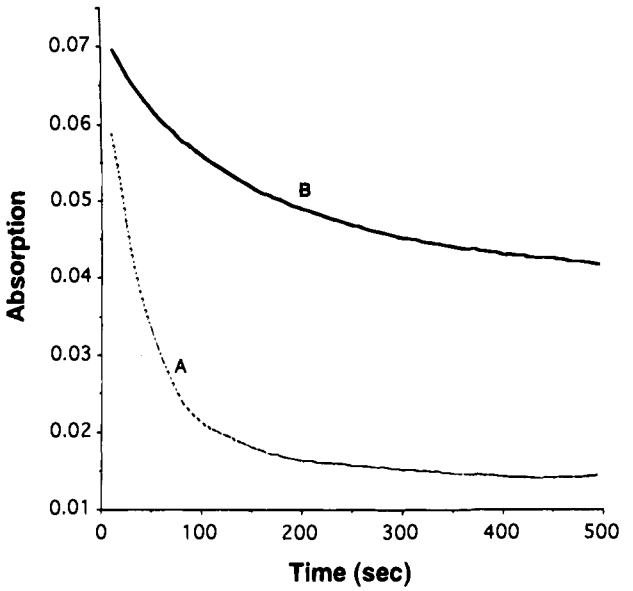

Figure 4. Time-dependent dissociation curves, followed at 642 nm, of $Co^{2+}-(13-30)$NCp7 (A) and $Co^{2+}-c[Glu^{17}, Lys^{30}(13-33)NCp7]$ (B) in the presence of 10 equiv of EGTA in 50 mM Hepes, 0.1 M KCl at pH 7.5 and 293 K.

(80 ms mixing times)[24] and NOESY experiments (200 ms mixing times)[25,26] were acquired using the TPPI method.[27] In each case, spectra were recorded with irradiation of the water resonance during the relaxation delay. All 2D spectra were processed using shifted sine-bell window functions in both dimensions. After zero-filling and double Fourier transformation, base line corrections were performed in both dimensions. The digital resolutions were 3.54 and 7.08 Hz per point in the F_2 and F_1 dimensions, respectively, by zero-filling once in the t_2 and twice in the t_1 dimension.

Structure Calculations. The proton–proton distance constraints were classified into three categories: 2.0–2.5, 2.0–3.5, and 2.0–4.5 Å corresponding to strong, medium, and weak NOEs, respectively. The zinc atom was parameterized as described elsewhere.[16] The cyclic structure was ensured by linking the side chain carboxylate of Glu^{17} and the ϵNH_2 of Lys^{30} through a covalent bond. The program DIANA[28] was run for structure calculations, by using the REDAC strategy as described by Güntert and Wüthrich.[29] The ten best structures obtained are then submitted to energy refinement by using AMBER.[30] Peptide bond parameters were assumed for the covalent bond between the side chains of Glu^{17} and Lys.[30] A zinc force field, obtained from *ab initio* calculation and parameterized in the AMBER framework, was used to account for the interactions between the zinc ion and the peptide ligands.

All structure calculations were performed on an IBM RISC System 6000-550 workstation. The computer graphic analysis and representations were obtained using the INSIGHT molecular modeling package (BIOSYM Technologies Inc, San Diego, CA) on a Silicon Graphics Iris R4400 workstation.

Results

Synthesis. In order to retain the three-dimensional structure of the native zinc finger (13–30)NCp7 in the NCp7, Asn^{17} and Ala^{30} were chosen as the cyclization sites, on the basis of structural modeling data.[16] These two residues were replaced by Glu^{17} and Lys^{30}, respectively, and the cyclization was performed between the side chains of the two amino acids (Figure 1). The sequence selected contains three additional residues at the C-terminal to facilitate the anchoring of the peptide on the resin and to prevent diketopiperazine formation

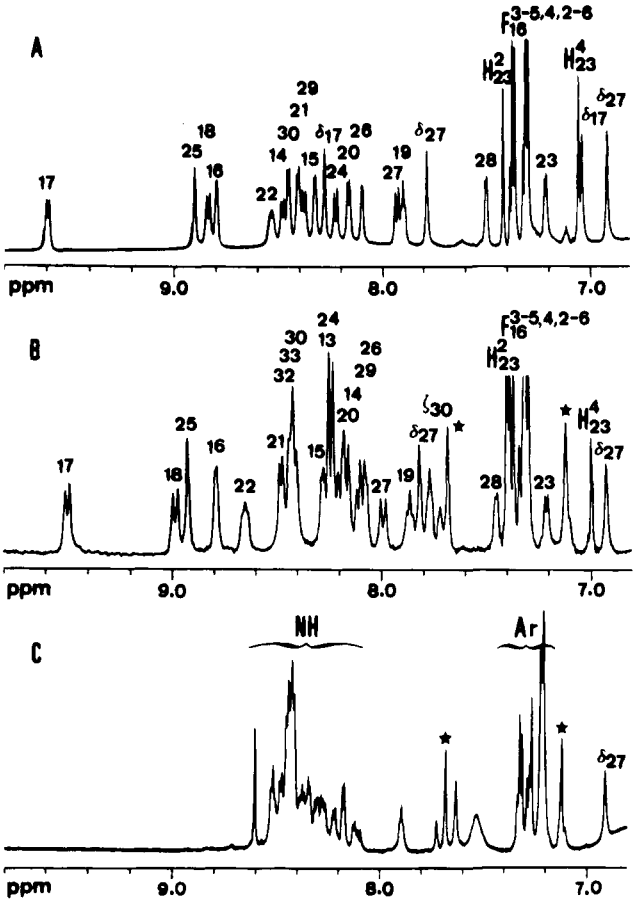

Figure 5. Part of the ^1H NMR spectra: (A), $Zn^{2+}-(13-30)$NCp7 (1.5:1); (B), $Zn^{2+}-c[Glu^{17}, Lys^{30}(13-33)NCp7]$ (1.5:1); (C), $Zn^{2+}-c[Glu^{17}, Lys^{30}(13-33)NCp7]$ in the presence of 9 equiv of EDTA in 90% H_2O and 10% D_2O at pH 5.6 ± 0.1 and 293 K. The ★ represents the C-terminal amide in the cyclic peptide.

(24) Griesinger, C.; Otting, G.; Wüthrich, K.; Ernst, R. R. *J. Am. Chem. Soc.* **1988**, *110*, 7870–7872.
(25) Jeener, J.; Meier, B. H.; Backmann, P.; Ernst, R. R. *J. Chem. Phys.* **1979**, *71*, 4546–4553.
(26) Macura, S.; Huang, Y.; Suter, D.; Ernst, R. R. *J. Magn. Reson.* **1981**, *43*, 259–281.
(27) Marion, D.; Wüthrich, K. *Biochem. Biophys. Res. Commun.* **1983**, *113*, 967–974.
(28) Güntert, P.; Braun, W.; Wüthrich, K. *J. Mol. Biol.* **1991**, *217*, 517–530.
(29) Güntert, P.; Wüthrick, K. *J. Biomol. NMR* **1991**, *1*, 447–456.
(30) Singh, U. C.; Weiner, P. K.; Caldwell, J.; Kollman, P. A. *AMBER* (UCSF Version 4.0); School of Pharmacy, University of California: San Francisco, CA, 1986.

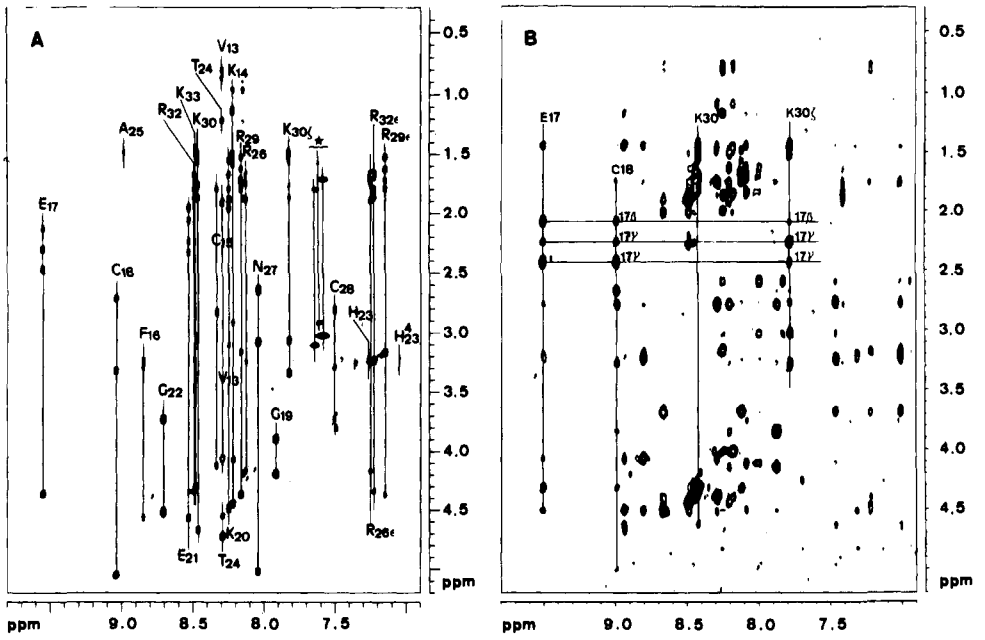

Figure 6. Part of (A) the TOCSY spectrum and (B) the NOESY spectrum of Zn^{2+}−c[Glu^{17}, Lys^{30}(13−33)NCp7] (1.5:1) in 90% H_2O and 10% D_2O at pH 5.5 and 293 K, with a mixing time of 80 ms for TOCSY and 200 ms for NOESY spectra. In (A) are shown the connectivities among the amide proton and its aliphatic protons (indicated by the residue number). In (B) are shown the NOE connectivities of the ζNH of the Lys^{30} with the side chain protons of the Glu^{17}, evidence for the cyclization between Glu^{17} and Lys^{30}.

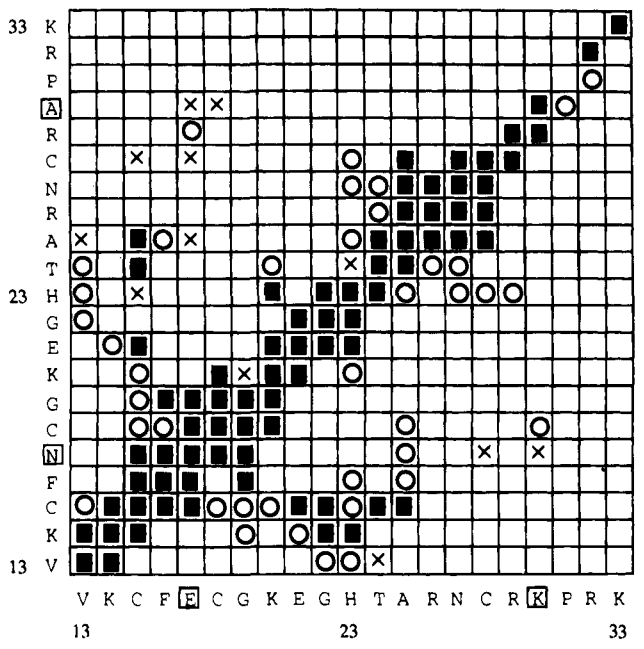

Figure 7. NOE pattern of native (13−30)NCp7 (above the diagonal) and its cyclic analog, c[Glu^{17},Lys^{30}(13−33)NCp7] (below the diagonal). Filled black squares (■) indicate NOEs between backbone protons, circles (○) indicate NOEs between backbone and side chain protons, and crosses (×) indicate NOEs between side chain protons. When two residues are connected by more than one NOE, only the one that involves the largest number of backbone protons is shown.

involving the proline residue. C- and N-terminals were protected respectively by amidation and acetylation from enzymatic degradation during immunization experiments.

The synthesis was designed in such a way that the two preselected amino acids could be specifically cyclized (Figure 2). For this purpose, a mixed "Fmoc and Boc" strategy was used. Firstly, the two amino acids were introduced in the peptide sequence with their side chains protected with "Fmoc-type" groups (*t*Bu and Boc) which could be deprotected by TFA treatment. The other amino acids were used as "Boc-type"-protected side chain forms, which were resistant to TFA, except His^{23} and Asn^{27} which were commercially available only as N(γ)- and N(τ)-trityl derivatives, respectively. Consequently, these two residues were also deprotected by TFA but did not disturb the cyclization step.[31] At the end of the synthesis, a treatment with TFA both deprotected the amino acids mentioned above and liberated the peptide from resin. The crude peptide was used for the cyclization step which was performed in solution. Finally, the remaining side chain protections were cleaved by HF, and the cyclic peptide was purified (final yield, 12%) and identified by mass spectroscopy (calcd, 2470.3; found, 2471) and amino acid analysis. NMR spectrum and HPLC analysis showed that the purity is ≥95%.

UV Measurements. The visible absorption spectra of Co^{2+}−(13−30)NCp7 and Co^{2+}−c[Glu^{17}, Lys^{30}(13−33)NCp7] (Figure 3) are characteristic of an almost symmetrical tetrahedral structure, as shown by the position and the intensity of the bands at 695, 642, and 615 nm.[5,9] The similarity of the two spectra indicates that both peptides coordinate cobalt ion in the same manner.

Addition of a 10-fold excess of EGTA in the 1/1 Co^{2+}−peptide complexes induced a slow decomplexation of the metallic ion (Figure 4). Interestingly, the optical density at 642 nm decreased more rapidly in the complex containing the normal zinc finger peptide than in that containing the cyclic one. This reflects a greater stability of the complex formed with the cyclic peptide than with the linear analog.

Encouraged by this preliminary result, we determined the affinity constants of Co^{2+} for the two peptides by titration experiments. Addition of increasing amounts of EGTA to various concentrations of Co^{2+}−peptide (1/1) complexes allowed the calculation of the apparent affinity constants of the complex Co^{2+}−(13−30)NCp7, K_{app} = 2.4 (±0.4) × 10^9 M^{-1} and that of the complex Co^{2+}−c[Glu^{17}, Lys^{30}(13−33)NCp7], K_{app} = 1.0 (±0.8) × 10^{10} M^{-1}.

NMR Studies. The aromatic and NH regions of the native (13−30)NCp7 in the presence of Zn^{2+} (A) and its cyclic analog

(31) Hoffmann, E.; Beck-Sickinger, A. G.; Jung, G. *Liebigs Ann. Chem.* **1991**, 585−590.

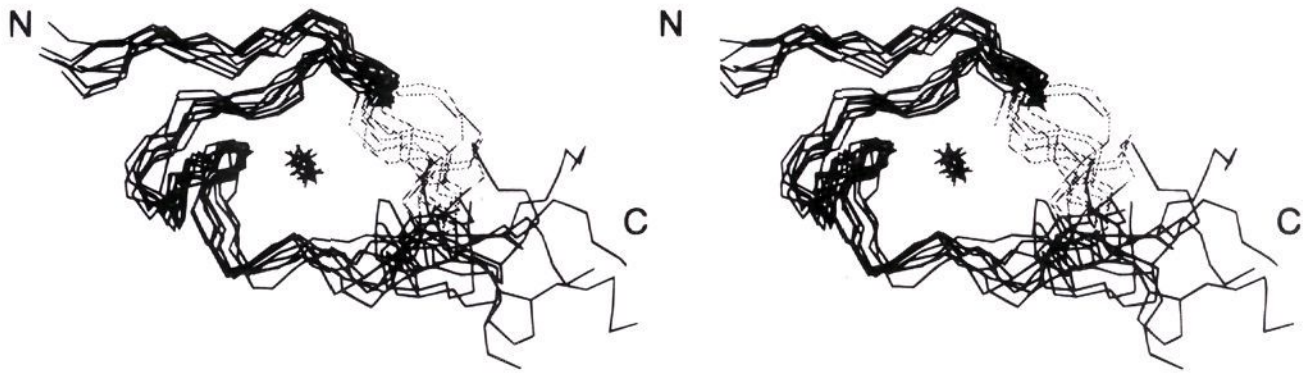

Figure 8. Stereoview of 10 best superimposed DIANA structures of the Zn^{2+}−c[Glu^{17}, Lys^{30}(13−33)NCp7]. The cyclization bond is shown with a dashed line.

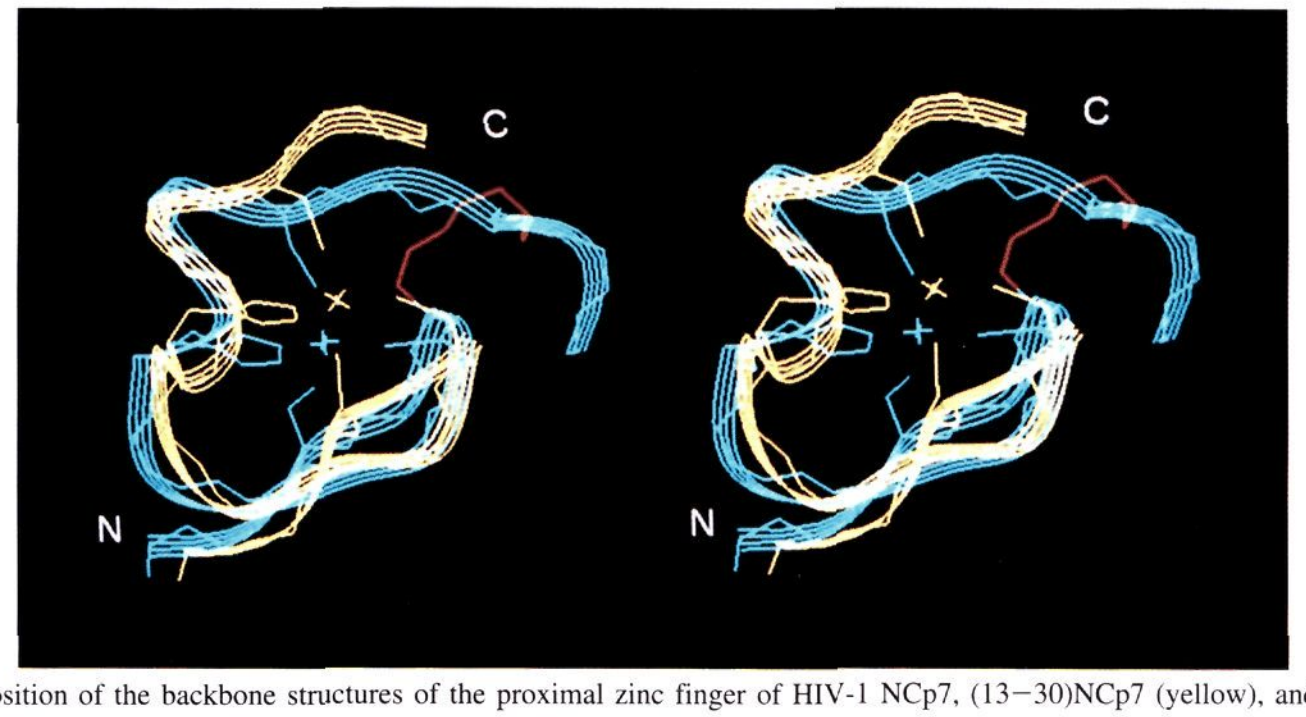

Figure 9. Superposition of the backbone structures of the proximal zinc finger of HIV-1 NCp7, (13−30)NCp7 (yellow), and its cyclic analog, c[Glu^{17}, Lys^{30}(13−33)NCp7] (blue). The cyclization bond is shown in red.

c[Glu^{17}, Lys^{30}(13−33)NCp7] in the presence of (B) and in the absence (C) of Zn^{2+} are compared in Figure 5. A great similarity between the spectra of both Zn^{2+}-complexed peptides is observed with a large scattering of the chemical shifts of the NH protons, evidence for the peptide backbone folding around the Zn^{2+} ion, and the unusual position of His^{23} imidazole protons which are deshielded by Zn^{2+} chelation.

The removal of Zn^{2+} by addition of an excess of EDTA (9 equiv) to the cyclic peptide led to a complete disappearance of the parameters characteristic of the folding of the peptide backbone (Figure 5C). This effect is well-correlated to that observed previously for NCp7 or its noncyclic zinc finger domains.[32]

The complete specific assignment of all protons was obtained using conventional strategies.[33] TOSCY spectra were used to delineate the spin systems corresponding to the different types of residues. The sequential assignments rely on the sequential NH−NH(i, i + 1) and Hα−NH(i, i + 1) connectivities and cross peaks observed in NOESY spectra.

To illustrate this assignment, a portion of the TOCSY spectrum of the cyclic peptide is presented in Figure 6A. This spectrum shows the connectivities between the amide groups and their corresponding aliphatic protons. Also clearly observed in this spectrum is the ζNH of Lys^{30} (Figure 6A, K30ζ), which gives a narrow resonance peak characteristic of an amide proton, unlike the ζNH_3^+ of the other lysines (Figure 6A, ★) which give relatively large resonances. The difference is evidence for the participation of Lys^{30} in cyclization. Further and stronger evidence is shown in part of the NOESY spectrum with the cross peaks between the β and γ protons of Glu^{17} and ζNH of Lys^{30} (Figure 6B), which reflect the correct cyclization of these amino acid side chains.

The direct comparison of the chemical shifts of each individual residue in the Zn^{2+}-complexed cyclic peptide and native peptide[34] (not shown here), emphasizes the analogies between the two compounds. Except for Glu^{17} and Lys^{30}, which are not present in the native (13−30)NCp7, the chemical shifts of all the other protons are nearly identical. The only significant shifts were observed for NH and α protons of Lys^{14}, Cys^{18}, Gly^{22}, and Arg^{29}. The maximal effect was found for Lys^{14} ($\Delta\delta$ = 0.29 ppm).

The global folding of the cyclic peptide in the presence of Zn^{2+} is very similar to that of the native peptide. The NOE pattern of the cyclic peptide exhibits the characteristic cross peaks of a retroviral-type zinc finger, just as its native analog (Figure 7): the relatively strong sequential NH_i and NH_{i+1} NOE contacts from Phe^{16} to Lys^{20} and from Ala^{25} to Cys^{28}, the NOE effects between $C^{\beta}H$ of Cys^{15} and the amide protons of Cys^{18}, Gly^{19}, Lys^{20}; the numerous spatial connectivities from the imidazole ring protons $C^{\delta 2}H$ and $C^{\delta 1}H$ of His^{23} to amide protons of Lys^{20}, Asn^{27}, Cys^{28}, and Arg^{29}. In contrast, the NOE effects between the backbone and side chain protons observed in the native peptide for Ala^{30} and Asn^{17} disappeared in the cyclic peptide, as expected.

Structure Description. The 231 interproton NOEs determined by ^1H NMR spectroscopy were introduced to the distance geometry program DIANA.[28] These constraints were separated into four groups: intraresidue effects (70 NOEs), sequential effects (71 NOEs), medium range (38 NOEs), and long range (52 NOEs) effects.

(32) South, T. L.; Blake, P. R.; Sowder, R. C., III; Arthur, L. O.; Henderson, L. E.; Summers, M. F. *Biochemistry* **1990**, *29*, 7786−7789.

(33) Wüthrich, K. *NMR of Protein and Nucleic Acids*; John Wiley & Sons: New York, 1986.

(34) Jullian, N.; Déméné, H.; Morellet, N.; Maigret, B.; Roques, B. P. *FEBS Lett.* **1993**, *331*, 43−48.

Figure 8 shows a superimposition of the 10 best conformations of the cyclic peptide obtained after best fit of the Cys^{15}–Cys^{28} backbone atoms, giving a root mean square deviation of 1.00 ± 0.05 Å. The total energy, after AMBER refinement, is about 88 ± 7 kcal mol^{-1}.

The Phe^{16}–Gly^{19} sequence is involved in a type I β-turn characterized by the following dihedral angle values for Glu^{17} ($\Phi = -56 \pm 10$, $\Psi = -61 \pm 12$) and Cys^{18} ($\Phi = -96 \pm 18$, $\Psi = -30 \pm 29$). The point mutation $Asn^{17} \rightarrow Glu$ induces some local distortion of the backbone conformation around residue 17: a type VII β-turn involves residues Cys^{15}–Cys^{18} in the native zinc finger. A type I β-turn is observed for residues Ala^{25}–Cys^{28} in both cyclic and native peptides. Nevertheless, the global folding of the C^{15}–C^{28} structure is conserved in the cyclic peptide: superimposition of the native peptide onto the cyclic peptide led to root mean square deviation around 1.4 Å for backbone atoms (Figure 9).

Discussion

The aim of this work was to prepare a cyclic analog of the proximal zinc finger peptide of HIV-1 NCp7, which could be used as a hapten to develop monoclonal antibodies against the authentic zinc finger(s) in the entire protein. For this purpose, a structural similarity between the cyclic and the linear native peptide was critical. It had been observed that the side chains of Asn^{17} and Ala^{30} in the proximal zinc finger are in close vicinity in the folded conformation of NCp7.[16] The distance between the two side chains being reasonable to attempt cyclization, Asn^{17} and Ala^{30} were replaced respectively by Glu^{17} and Lys^{30} which allowed an intramolecular stable amide bond to be formed.

The c[Glu^{17}, Lys^{30}(13–33)NCp7] peptide was synthesized by solid phase peptide synthesis. After removal of the lateral chain protections of Glu^{17} and Lys^{30} and cleavage of the peptide from the resin, the cyclization was achieved by a liquid phase method. The remaining side chain protecting groups were removed by treatment with HF. The final product was purified by HPLC.

The ability of the cyclic peptide to chelate metallic ions was explored by studying the formation of the stable tetragonal complex with Co^{2+} by visible spectroscopy. Firstly, it was observed that the native and cyclic peptides have similar visible absorption spectra in the presence of 1 equiv of Co^{2+}, and both spectra are characteristic of an almost symmetrical tetrahedral structure.[9] This indicates that both peptides complex a divalent metal in a similar manner. More interestingly, as expected on entropic grounds, the cyclic peptide was shown to have a higher affinity for Co^{2+} than the linear peptide. The calculated affinity constants of the corresponding complexes are 2.4×10^9 M^{-1} and 1×10^{10} M^{-1} for (13–30)NCp7 and its cyclic analog, respectively. The affinity constants of the two peptides for the zinc ion were not determined in this work since a good correlation was observed between the affinities of finger domains for zinc and cobalt ions.[9] It could therefore be assumed that the cyclic peptide has a higher affinity for Zn^{2+} than the native peptide.

The tridimensional structure of the cyclic peptide was studied in aqueous solution by ^1H NMR spectroscopy. In the absence of Zn^{2+}, the spectrum does not indicate the existence of a well-organized structure (Figure 5C). Conversely, in the presence of $ZnCl_2$ (1.5 equiv) a large dispersion of the NH resonances reflects the formation of the complex. The comparison of the NMR parameters (chemical shifts and NOEs) of the native and cyclic peptides indicates large analogies between their conformation. The superimposition of the modeled structures (Figure 9) shows a close overlap of the backbone atoms from Cys^{15} to Cys^{28}. This should favor obtaining antibodies directed against the finger but not necessarily toward the conformational epitope corresponding to the internally folded conformation of NCp7. In line with this it is important to observe that, in this spatial arrangement, the structure of the zinc finger does not differ from that found in an isolated CCHC array,[16,17,34] and only a small region of the fingers is in contact.

In conclusion, the structural characteristics exhibited by the cyclic analog of the (13–30)NCp7 domain show large analogies with the native peptide and an enhanced affinity for metallic ions which are favorable parameters for the production of antibodies against the zinc finger. Furthermore, the approach used in this work could be extended to the synthesis of a rigid analog of the entire NCp7 sequence, exploiting the spatial proximity between the Ala^{25} and Lys^{38} residues belonging to each zinc finger. Such a molecule could allow the biological role of Phe^{16} and Trp^{37}, found in proximity in NCp7, to be explored in detail. Immunization experiments are now in progress.

Acknowledgment. Thanks are due to Mrs. C. Dupuis for her assistance in drafting the manuscript and to Dr. Y. Mély for his helpful discussion in the affinity constant calculation. This work was supported by the French program against AIDS (ANRS).

JA942058H